Economic Geology
Vol. 85, 1990, pp. 1010–1023

Lateritic Weathering of Pyroxenites at Niquelandia, Goias, Brazil: The Supergene Behavior of Nickel

F. COLIN,

ORSTOM, 213 rue La Fayette, 75480, Paris Cedex 10, France, and Laboratoire de Geosciences des Environnements Tropicaux, case 431, U.A. du C.N.R.S. no. 132, Universite Aix-Marseille III, Faculté des Sciences de St.-Jerome, 13397 Marseille Cedex 13, France

D. NAHON,

Laboratoire de Geosciences des Environnements Tropicaux, case 431, U.A. du C.N.R.S. no. 132, Université Aix-Marseille III, Faculté des Sciences de St.-Jerome, 13397 Marseille Cedex 13, France

J. J. TRESCASES,

Laboratoire de Petrologie de la Surface, U.A. du C.N.R.S. no. 721, Université de Poitiers, 86022 Cedex, France

AND A. J. MELFI

Universidade de Sao Paulo, Instituto Astronomico e Geofisico, Av. Miguel Stefano, 4200, Caixa Postal 30.627, 01000 Sao Paulo, SP Brazil

Abstract

Two typical lateritic weathering profiles (Jacuba and Angiquinho) from the Niquelandia Ni deposits, Brazil, were studied in order to establish the petrological relationship between the supergene Ni products and the parental pyroxenes. From the base to the top of the profiles, pyroxenes are replaced by goethite and kaolinite through a series of transitional Ni-bearing phyllosilicates. The mineralogy and the chemical composition (especially the Ni content) of these clay minerals depends on the degree of fracturing and serpentinization of the pyroxenite and the location of the pyroxenite with respect to neighboring dunite. Within the Jacuba profile, smectite and pimelite pseudomorphs after pyroxene are especially Ni rich, and in fact, are the most Ni-enriched clay minerals now known in lateritic weathering profiles.

Introduction

THE Niquelandia area is located in the State of Goias, Brazil, 200 km north of Brasilia. In this area, lateritic weathering of ultramafic rocks has formed important nickel reserves (60×10^6 tons of 1.45% Ni; Pedroso and Schmaltz, 1981) that are now being mined. Two companies share the mining reserves: Codemin in the northern part and Niquel Tocantins cie. des Mines in the southern part. The area mined by Niquel Tocantins contains the Jacuba, Coriola, Angiquinho, Corrego da Fazenda, Vendinha, and Riberao do Engenho deposits and has reserves of 33 millions tons averaging 1.45 percent Ni.

These ores are not only derived from the weathering of dunite and peridotite, as are most of the world's nickeliferous laterite deposits (Golightly, 1981), but some have formed from the weathering of pyroxenite. The most characteristic Ni-bearing mineral present is Ni-rich smectite (Decarreau et al., 1987), which is not generally observed in most of the world's other lateritic nickel deposits. This study examines the main mineralogical and petrological characteristics of the weathering mantle covering these pyroxene-rich ultramafic rocks in order to determine the behavior of nickel during chemical weathering in this environment.

Several profiles exposed in strip mines and test pits were studied. Detailed examinations were performed on two vertical profiles from the Jacuba and Angiquinho deposits. Respectively, these are underlain by pyroxenite and by pyroxenite and dunite.

Field descriptions were supplemented with the study of oriented samples by optical microscopy, X-ray diffraction (XRD), and scanning electron microscope (SEM). The most Ni-rich smectites were studied by transmission electron microscopy (TEM), infrared optical absorption (IR), Mössbauer, and extended X-ray absorption fine-structure spectroscopy (EXAF) (Decarreau et al., 1987). Bulk chemical analyses were obtained using atomic absorption techniques on samples of 3-kg size. The chemical composition of minerals was obtained by extensive electron microprobe analysis (Colin, 1985). The results of these analyses have been published (Colin, 1985) and, therefore, only the average structural formulas of compositionally similar phases are used here.

0361-0128/90/1084/1010-14$3.00

Climate and Vegetation

The climate in the Niquelandia area is tropical with a six-month rainy season. Mean annual rainfall is about 150 cm and the average temperature is about 23°C. The area is a rolling forested upland with scattered grassy areas that in Brazil are called "Cerrado." The grass lands are characterized by a population of graminaceae plants, the occurrence of one species (Velosia compacta) identifies the presence of pyroxenite (A. C. Pedroso, pers. commun., 1984).

Geology and Geomorphology

The Niquelandia igneous body is about 40 km long and 20 km wide. It extends north-northeast from the village of Niquelandia (Fig. 1) and is of Archean or Proterozoic age (Girardi et al., 1978). No regular foliation of the rocks has been observed and the dips of layering range from 40° to 60° (Girardi et al., 1986). The complex consists of a lower and an upper sequence (Araujo et al., 1972; Figueiredo et al., 1975; Leonardos et al., 1982; Rivalenti et al., 1982). The

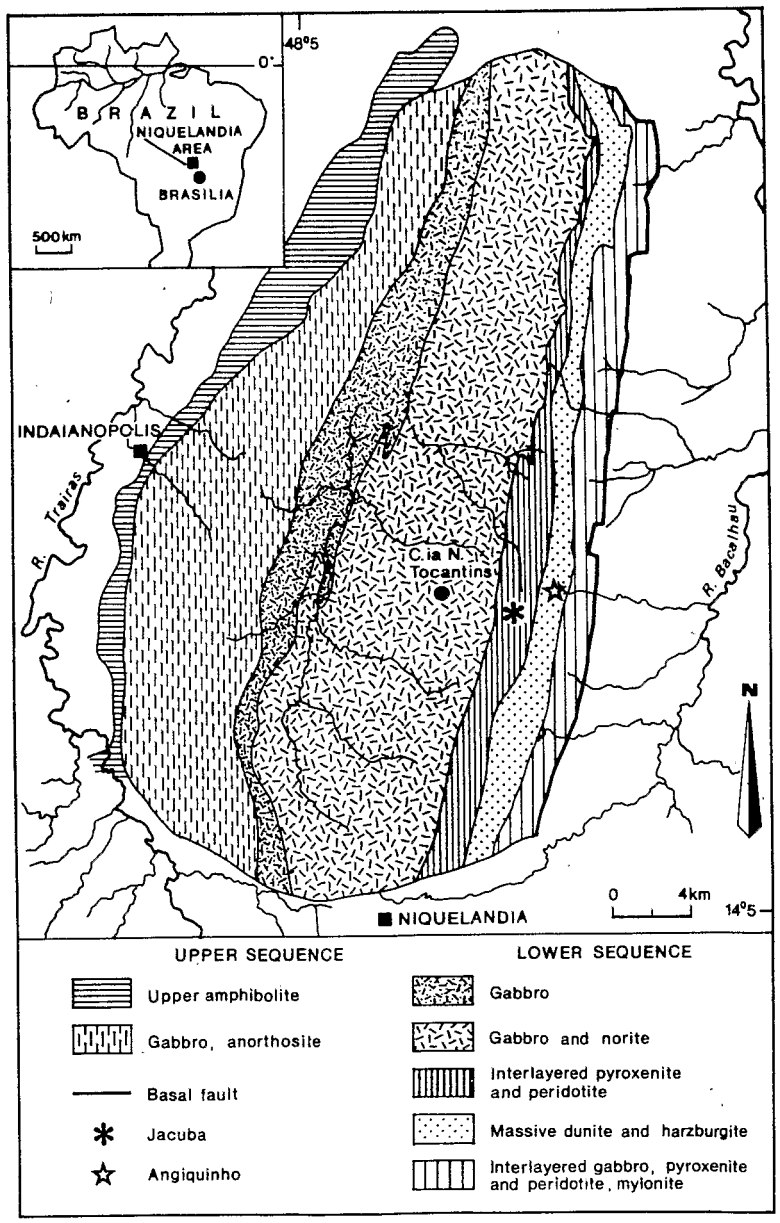

FIG. 1. Generalized geology of the Niquelandia complex (after Girardi et al., 1986).

lower sequence is composed of a basal layered zone of gabbro, peridotite, and pyroxenite that is overlain by an ultramafic zone of peridotite and pyroxenite. This is, in turn, overlain by layered gabbros (Girardi et al., 1986). The upper sequence consists of gabbro, anorthosite, and upper amphibolite (Fig. 1).

The lower sequence is in tectonic contact with older metamorphic rocks (gneiss, quartzite, and amphibolite) that constitute the Archean basement (Danni et al., 1982). Rivalenti et al. (1982) have shown that mafic and ultramafic rocks from the lower sequence are intrusions and formed by fractional crystallization of a basaltic magma. Rivalenti et al. (1982) and Girardi et al. (1986) report that the entire Niquelandia body represents a single igneous complex and that the lower and upper sequence are comagmatic.

The ultramafic units of the lower sequence form the "Serra da Mantiqueira" area where elevations range up to 1,100 m. Dunites and partially serpentinized harzburgites, with some podimorph chromite bodies, occur in the eastern part of this area, while interlayered peridotite and pyroxenite underlie the western part (Fig. 1). The Angiquinho deposit is located in the eastern part of the Serra da Mantiqueira, is underlain by dunites and lenses of partly serpentinized pyroxenites, and is capped by a ferricrete crust that is locally called "Canga." In contrast, the Jacuba deposit is located to the west, is underlain mostly by fresh pyroxenite, and is capped by a silcrete formation. Between these two deposits is a valley carved in pyroxenites (Fig. 2) (Pecora, 1944; Melfi et al., 1980).

Weathering Profiles

The Jacuba profile

The profile of Jacuba is formed by the weathering of pyroxenite. The profile is up to 30 m thick and consists of four main layers (Fig. 3). The chemical data of the parent rock and of the layers are given in Table 1.

At the bottom, the 7-m-thick coherent layer represents the earliest stages of weathering. Rocks in this layer vary from greenish-black to beige in color and have densities that decrease from fresh rock values of 3.8 to values of 2.0. Although the rock is coherent, it is cut by a network of cracks filled with garnierite (kerolite-pimelite series) and greenish smectite. These cracks formed along tectonically induced joints. The weathered rock between these cracks consists of enstatite and diopside that are partly altered to smectite. However, the smectite is not well developed except where the parent rock is strongly fractured. Because the original structures are well preserved, the weathering in this layer have been isovolumetric.

Mass balance calculations show that 60 to 90 percent of MgO, 40 to 50 percent of SiO_2, 0 to 80 percent of CaO, and about 40 percent of the Al_2O_3 have been removed. Cr_2O_3 has been immobile. In contrast, NiO shows an increase ranging from 1,080 to 5,560 percent.

The overlying saprolitic layer develops from further weathering of the fractured bed rock. It is browner, thicker (8 m), and more friable than the underlying coherent layer. Also, the residual joint-bounded blocks become rounder and decrease in size upward. Between blocks, the greenish matrix is cut by centimeter- to millimeter-thick cracks that are filled with greenish smectite and garnierite. Some cracks contain asbolane. Toward the top of this layer only a few small pieces of brownish rocks persist and are scattered in a green-brown clayey matrix. The density of this matrix is about 1.3 and it still preserves the original rock structures.

The chemical trend is the same as in the underlying layer. There is a 70 percent loss of SiO_2, a 60 percent loss of CaO, and an 80 percent loss of MgO; in contrast, the NiO content is enriched about 2,100 percent over the amount in the parent rock.

The clayey layer is 8 m thick and contains no residual bed-rock fragments. It is composed of green-brown smectite with reddish ferruginous pseudomorphs after 1-mm-long pyroxenes. Most cracks are

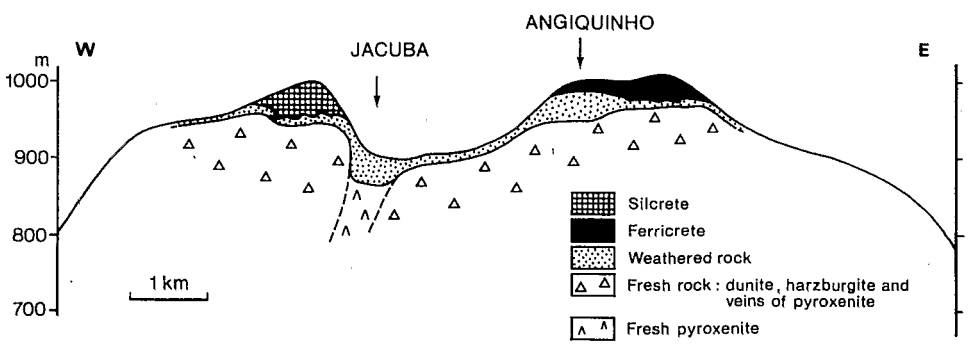

FIG. 2. Cross section of Jacuba and Angiquinho deposits.

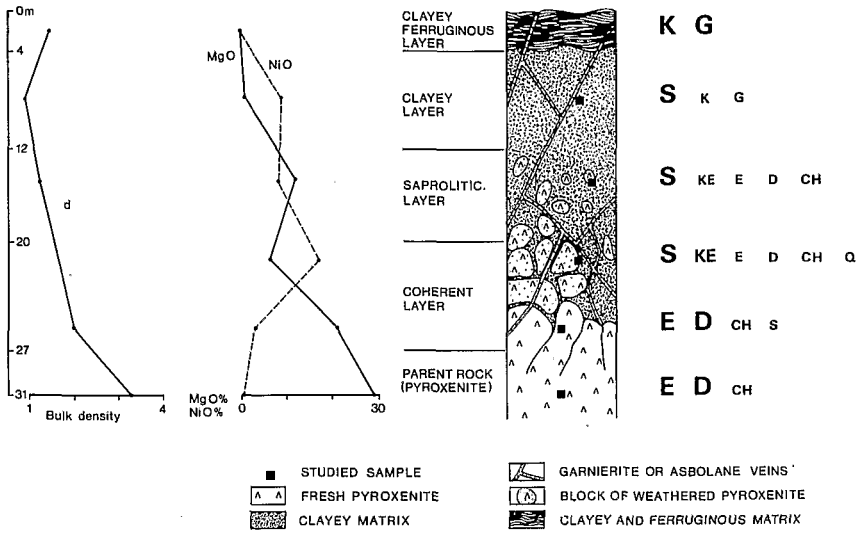

FIG. 3. The Jacuba weathering profile. Mineralogic and chemical data. CH = chromite, D = diopside, E = enstatite, G = goethite, K = kaolinite, KE = kerolite, Q = quartz, S = smectite; large letters = very abundant, medium letters = abundant, small letters = less abundant.

filled with asbolane (Co-Mn-Ni oxides). CaO and MgO have been almost completely removed; 80 percent of the SiO_2 has been leached. Although the NiO content is 1,420 percent higher than in the parent rock, it is less than in the underlying layer.

The clayey ferruginous layer is 4 m thick and consists of reddish to whitish, variegated clay-sized goethite and kaolinite. This part of the profile has been compacted so that the primary structure of the parent rock has been destroyed. A mass balance calculation, based on the assumption that Cr_2O_3 has been immobile, indicates that Al_2O_3 has remained constant but that Fe_2O_3 has been introduced. The NiO content in this layer is low, with a loss of 80 percent relative to the parent rock.

The Angiquinho profile

The weathering profile at Angiquinho formed on a combination of dunite and partially serpentinized pyroxenite, a parent that contrasts with the pyroxenite which forms the base of the Jacuba profile. This 40-m-thick profile is thicker than the one at Jacuba and consists of five layers (Fig. 4). The chemical data of the parent rock and of the layers are given in Table 2.

The 13-m-thick beige-colored coherent layer is at the bottom. Rock in this zone has a bulk density of 2.01, which is less than the 2.67 of the parent rock. A dense network of nearly horizontal cracks that are one to a few centimeters thick cuts this layer. Where the pyroxenite is strongly serpentinized, the cracks

TABLE 1. Bulk Chemical Data and Mass Balance Calculations for Layers of the Jacuba Weathering Profile

Layer	Parent rock	Coherent layer weakly fractured	Δ %	Coherent layer strongly fractured	Δ %	Saprolitic layer	Δ %	Clayey layer	Δ %	Clayey ferruginous layer	Δ %
SiO_2	54.00	50.64	−40	53.72	−50	44.14	−70	42.70	−80	16.58	−90
MgO	29.00	21.10	−60	6.42	−90	11.81	−80	1.82	−98	0.30	−99
CaO	4.06	6.65	0	1.68	−80	4.06	−60	0.00	−100	0.01	−99
Fe_2O_3	8.40	9.83	−30	9.10	−40	11.62	−45	21.30	−30	57.20	+90
Al_2O_3	3.16	3.49	−30	3.35	−45	5.67	−30	8.22	−30	11.33	0
CR_2O_3	0.37	0.57	−5	0.60	−15	1.32	+40	2.62	+95	1.31	0
MnO_2	0.22	0.20	−45	0.21	−50	0.15	−70	0.42	−50	0.57	−30
NiO	0.16	3.10	1,080	17.43	5,560	8.74	2,100	8.81	1,420	0.11	−80
CoO	0.01	0.02	0	0.08	320	0.05	100	0.13	260	0.02	−40
CuO	0.05	0.31	280	0.75	680	1.25	900	1.04	480	0.52	200
H_2O	0.17	2.26	710	6.61	1,920	6.67	1,470	9.97	1,520	7.30	1,110
d	3.26	1.99		1.69		1.31		0.90		1.51	

Data are in wt percent; calculations (Δ %) show compositional changes are relative to the parent rock; d = bulk density

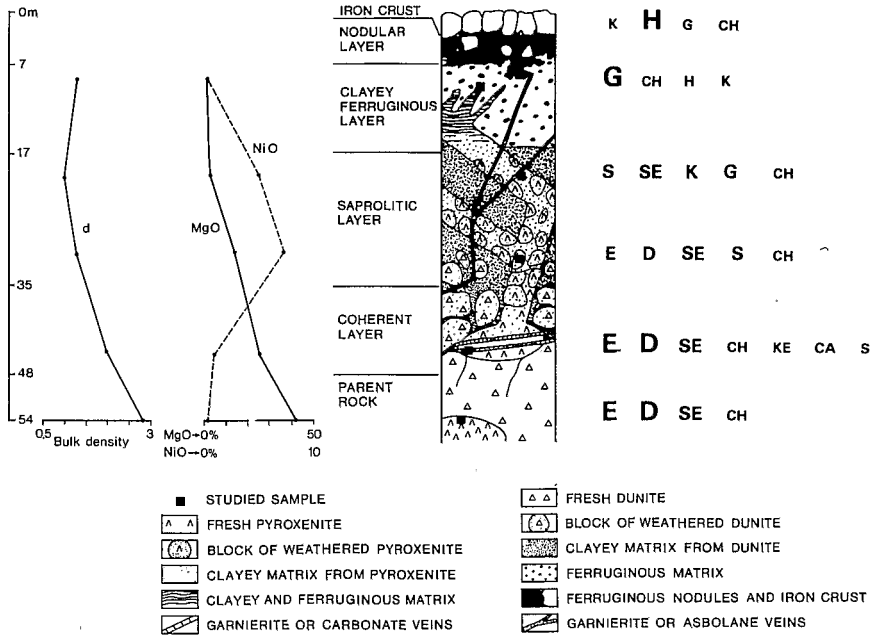

FIG. 4. The Angiquinho weathering profile. Mineralogic and chemical data. CA = carbonate, CH = chromite, D = diopside, E = enstatite, G = goethite, H = hematite, K = kaolinite, KE = kerolite, S = smectite, SE = serpentine; large letters = very abundant, medium letters = abundant, small letters = less abundant.

are filled with dolomite and magnesite; where the pyroxenite is unaltered or slightly serpentinized, the cracks contain garnierite.

Chemical patterns in the coherent layer are similar to those in the coherent layer at Jacuba. Mass balance calculations indicate that about 50 percent of the MgO and 20 percent of the SiO_2 have been removed. On the other hand, NiO shows an enrichment of 190 percent over the value in the parent rock. The amounts of MgO and SiO_2 depletion and NiO enrichment are not as great as those observed at Jacuba, where the parent rock was not serpentinized. The abundances of the other elements indicate that they have been neither increased nor depleted.

In the 18-m-thick saprolitic layer, blocks of dunite are changed into a reddish clayey rock. The size and abundance of reddish blocks decrease upward until distinguishable fragments of weathered dunite are absent at the top of the layer. On the other hand, blocks of weathered pyroxenite persist throughout

TABLE 2. Bulk Chemical Data and Mass Balance Calculations for Layers of the Angiquinho Weathering Profile

Layer	Parent rock	Coherent layer	Δ %	Saprolitic layer bottom	Δ %	Saprolitic layer top	Δ %	Clayey ferruginous layer	Δ %
SiO_2	37.08	40.98	−20	42.22	−45	46.66	−50	4.30	−98
MgO	40.60	26.11	−50	16.16	−80	3.73	−95	0.50	−99
CaO	0.41	0.02	−95	0.03	−95	0.04	−95	0.00	−100
Fe_2O_3	8.22	14.46	30	9.10	−45	21.95	0	72.60	15
Al_2O_3	0.26	1.49	330	6.33	1,075	1.60	135	5.67	190
Cr_2O_3	0.56	0.75	0	0.79	−30	1.08	−25	4.26	0
MnO_2	0.15	0.25	25	0.37	20	0.47	20	0.20	−80
NiO	0.30	1.14	190	7.47	1,100	5.26	570	0.75	−70
CoO	0.01	0.02	50	0.08	285	0.81	2,990	0.02	−70
CuO	0.01	0.01	−25	0.03	45	0.06	130	0.05	−30
H_2O	12.78	12.82	−25	13.74	−50	17.86	−50	11.70	−90
d	2.67	2.01		1.29		1.02		1.35	

Data are in wt percent; calculations (Δ %) show compositional changes are relative to the parent rock; d = bulk density

this layer and preserve primary bed-rock structures. The pyroxenites are progressively replaced by a green clayey saprolite which is very different from the reddish weathered products developed around dunite. The same system of cracks that was observed in the coherent layer occurs in this part of the profile, but here the cracks are filled with Co-Mn-Ni oxides.

Mass balance calculations show that, relative to the parent rock, 50 percent of the SiO_2 and 80 to 95 percent of the MgO have been lost; within this layer, NiO shows a gain ranging from 1,100 percent (bottom) to 570 percent (top).

The clayey ferruginous layer is 10 m thick and consists of reddish saprolite (goethite), which developed from the weathering of dunite, and of purple-whitish saprolite (goethite-kaolinite), which formed from the weathering of pyroxenite. Compaction has destroyed all primary bed-rock structures. Mass balance calculations made assuming a constant content of Cr_2O_3 indicates a gain in Al_2O_3 and a significant loss of NiO.

The nodular layer is a 4-m-thick zone made up of a powdery red ferruginous material (goethitic nodules).

The uppermost part of the profile is a 3-m-thick iron crust (Canga). It consists of hard ferruginous blocks of hematitic crust with a nodular facies.

Weathering of Pyroxenites—Petrological Patterns

Parent rocks

Data from both the Jacuba and Angiquinho profiles provide information on the weathering of pyroxenites. The parent rock of both profiles is a finely granular pyroxenite which consists of approximately two-thirds partly altered orthopyroxenes (enstatite) and one-third clinopyroxenes (diopside) (Fig. 5A). Average formulas of these minerals are: enstatite: $(Si_{1.974}Al_{0.026})(Al_{0.028}Fe^{+2}_{0.273}Mg_{1.657}Ni^{+2}_{0.001}Cr^{+3}_{0.014}Ti^{+4}_{0.001}Ca_{0.009}Mn^{+2}_{0.007})O_6$, and diopside: $(Si_{1.968}Al_{0.032})(Al_{0.036}Fe^{+2}_{0.087}Mg_{0.882}Cr^{+3}_{0.024}Ti^{+4}_{0.006}Ca_{0.924}K_{0.035}Mn^{+2}_{0.004})O_6$. The parent pyroxenes at Jacuba are never serpentinized, but those at Angiquinho are weakly to strongly serpentinized. In strongly serpentinized rock, granular pyroxenes are pseudomorphically replaced by lizardite with a bastite texture. These bastites are embedded by a network of serpentine with a mesh texture (Fig. 5B) as described by Wicks and Whittaker (1977) and Dungan (1979a and b). The average formulas obtained for serpentine minerals are bastites: $(Si_{1.967}Al_{0.030}Fe^{+3}_{0.003})(Al_{0.080}Fe^{+2}_{0.369}Fe^{+3}_{0.051}Mg_{2.430}Cr^{+3}_{0.011}Ni^{+2}_{0.005})O_5(OH)_4$, and "mesh" serpentines: $(Si_{1.932}Al_{0.005}Fe^{+3}_{0.063})(Al_{0.001}Fe^{+2}_{0.177}Fe^{+3}_{0.076}Mg_{2.729}Ni^{+2}_{0.013})O_5(OH)_4$. The chemical composition of the mesh serpentine, low in Al_2O_3 and Cr_2O_3 (Fig. 6) and high in nickel, indicates that these serpentines result from the replacement of olivine (Golightly and Arancibia, 1979).

Weathering transition from the parent rock to the coherent layer

The first indications of pyroxenes weathering at both the Jacuba and Angiquinho profiles develop along boundaries between mineral grains and within intramineral cracks. SEM imagery shows that, along cracks, surfaces of pyroxene grains show dissolution voids similar to those described by Berner et al. (1980) and Berner and Schott (1982). The products of this first stage of dissolution are observed on the surfaces of nearby pyroxenes and consist of an authigenic goethite (avg 1% Ni) which occasionally occurs as rosette-forming laths (Fig. 5C). In contrast, serpentines, which are only present at Angiquinho, remain unaltered during the first stage of weathering.

Weathering evolution from the coherent layer to the clayey layer at Jacuba

The coherent layer may be cut by numerous fractures. Where fractures are relatively sparse, 50- to 150-μ-wide zones of smectite alteration occur along edges of cracks that occur in enstatites and diopsides (Fig. 5D and E). Electron microprobe analyses indicate that two compositional types of smectites (Fe saponite) occur (Fig. 7). Their average compositions are: type 1: $Si_{3.222}Al_{0.752}Fe^{+3}_{0.026})(Al_{0.030}Fe^{+3}_{0.936}Mg_{0.222}Ni^{+2}_{1.529}Cr^{+3}_{0.078}Ti^{+4}_{0.007})(Ca_{0.054}K_{0.007})O_{10}(OH)_2$, and type 2: $(Si_{3.420}Al_{0.473}Fe^{+3}_{0.107})(Fe^{+3}_{1.176}Mg_{0.290}Ni^{+2}_{1.070}Cr^{+3}_{0.001}Ti^{+4}_{0.003})(Ca_{0.076}K_{0.003})O_{10}(OH)_2$. In the first type, Ni occupies 46 percent of the octahedral sites, but it occupies only 34 percent of those sites in the second type. For this reason, it is likely that smectites of the second type were derived from those of the first.

Where the coherent layer is cut by numerous fractures, smectite replacement is much more extensive and fills embayments developed at the expense of pyroxenes (Fig. 5F). These phyllosilicates form pseudomorphs after tooth-shaped pyroxenes (Fig. 8A). X-ray diffraction and microprobe analyses show that this matrix is composed of a mixture of two-thirds Fe saponite and one-third pimelite. Average formulas for these phases are: Fe saponite: $(Si_{3.796}Al_{0.204})(Al_{0.235}Fe^{+3}_{0.767}Mg_{0.464}Ni^{+2}_{1.002}Cr^{+3}_{0.064}Ti^{+4}_{0.010})(Ca_{0.017})O_{10}(OH)_2$, and pimelite: $(Si_4)(Al_{0.010}Fe^{+3}_{0.174}Mg_{0.156}Ni^{+2}_{2.520}Cr^{+3}_{0.013}Ti^{+4}_{0.008}Ca_{0.009}K_{0.007})O_{10}(OH)_2$. Ni occupies 32.5 percent of the octahedral sites in the Fe saponite and 84 percent in the pimelite.

From the base to the top of the saprolitic layer, the phyllosilicates replace an increasing proportion of the pyroxene; however, the texture of the parent pyroxenite is still preserved (Fig. 8B). In the final stage, the phyllosilicate matrix has centripetally re-

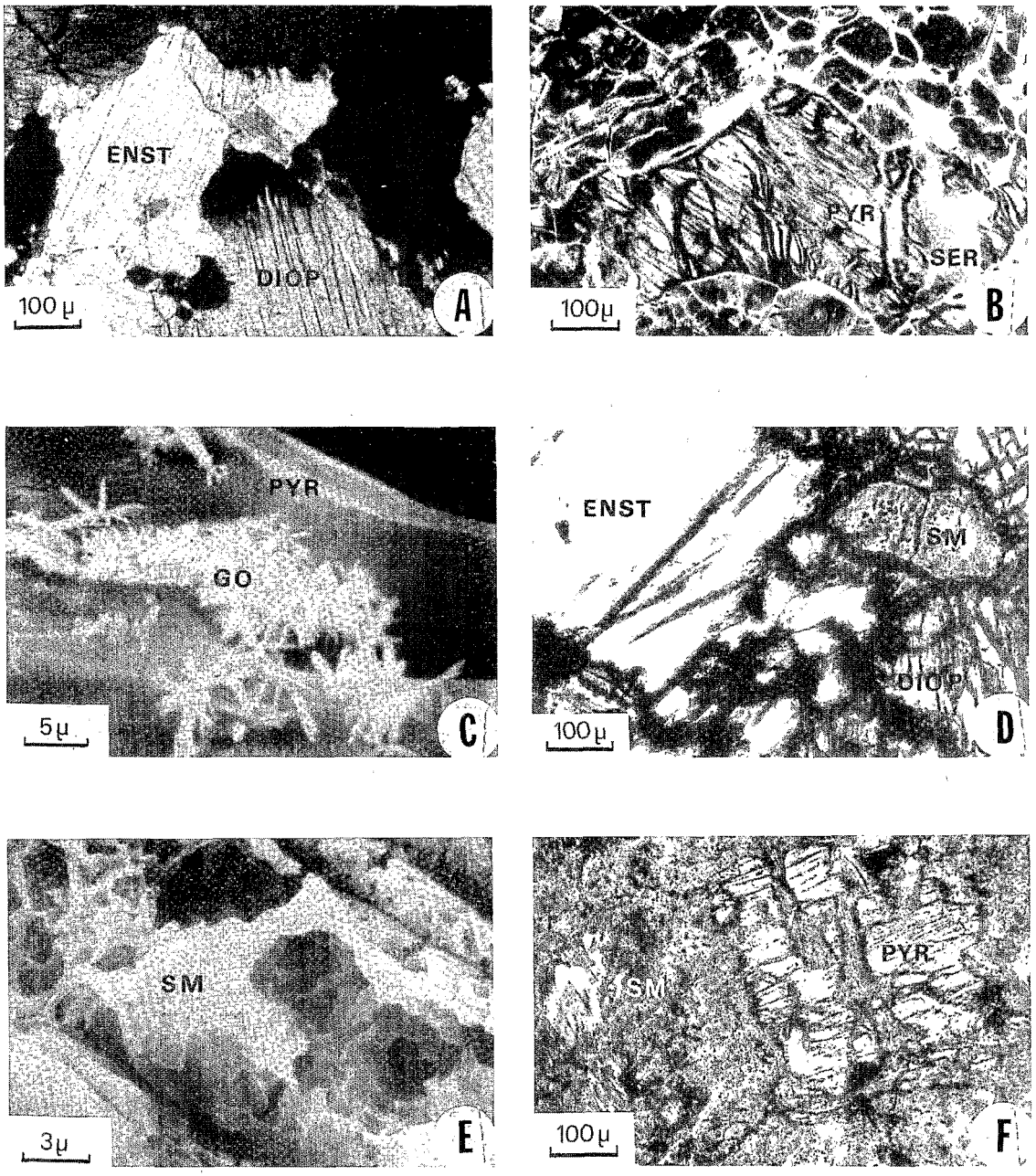

FIG. 5. A. Unweathered parent enstatite (ENST) and diopside (DIOP). Thin section under crossed polars. B. Serpentine (SER) pseudomorph after pyroxene (PYR). Thin section under crossed polars. C. Epitaxic goethite (CO) on tooth-shaped pyroxene (PYR). Scanning electron photomicrograph. D. Weathering of enstatite (ENST) and diopside (DIOP) into smectite (SM). Thin section under crossed polars. E. Smectite (SM) with honeycomb structure. Note the preservation of parent mineral texture. Scanning electron photomicrograph. F. Weathering of pyroxene (PYR) into smectite (SM). The phyllosilicate matrix cuts up the parent minerals. Thin section under crossed polars.

placed every pyroxene and consists of Ni saponite and Fe-Al saponite (Fig. 9). Average formulas for these phases are: Ni saponite: $(Si_{3.671}Al_{0.325}Fe^{+3}_{0.004})(Al_{0.100}\ Fe^{+3}_{0.354}\ Mg_{0.121}\ Ti^{+4}_{0.009}\ Ni^{+2}_{2.138}\ Cr^{+3}_{0.093}\ Cu^{+2}_{0.031})(Ca_{0.013}\ K_{0.047})O_{10}(OH)_2$, and Fe-Al saponite: $(Si_{3.660}\ Al_{0.335}\ Fe^{+3}_{0.005})\ (Al_{0.346}\ Fe^{+3}_{0.540}\ Mg_{0.173}\ Ti^{+4}_{0.013}\ Ni^{+2}_{1.263}\ Cr^{+3}_{0.175}Cu^{+2}_{0.046})(Ca_{0.036}K_{0.065})O_{10}(OH)_2$. The smectites formed in the center of the pyroxene are Ni saponites, with Ni occupying 68 percent of the octahedral sites. Smectites on the pyroxene rims are a mixture of 30

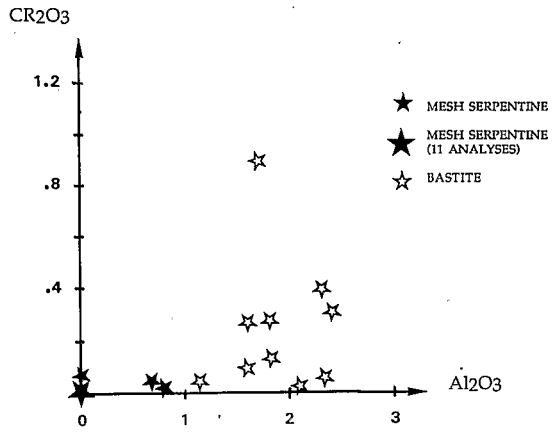

FIG. 6. Cr_2O_3 and Al_2O_3 variations in bastite and mesh serpentine from the coherent layer at Angiquinho.

percent Ni saponites and 70 percent Fe-Al saponites in which Ni occupies 41 percent of the octahedral sites.

The overlying clayey layer is cut by cracks filled with dark asbolane that averages 19 percent Ni. All relict pyroxenes are gone, although the texture of the parent rock is still preserved (Fig. 8C). Nickeliferous ferruginous oxyhydroxides (avg 4% Ni; Fig. 8C) are disseminated in a yellow-green clay matrix. Fe-Al saponites in this layer occur in the cores and on the rims of the relict pyroxenes and have an average formula of: Fe-Al saponite: $(Si_{3.767}Al_{0.233})(Al_{0.485}Fe^{+3}_{0.725}Mg_{0.179}Ti^{+4}_{0.012}Ni^{+2}_{0.902}Cr^{+3}_{0.098})(Ca_{0.020}K_{0.059})O_{10}(OH)_2$. Ni occupies 29 percent of the octahedral sites. This saponite occurs with beidellite and kaolinite in the cores of pyroxenes and with hisingerite on pyroxenes rims; the hisingerite is similar to that studied by Brigatti (1981) and Paquet et al. (1983). Average formulas for these two phases are: beidellite: $(Si_{3.684}.Al_{0.316})(Al_{0.643}Fe^{+3}_{0.687}Mg_{0.214}Ti^{+4}_{0.016}Ni^{+2}_{0.623}Cr^{+3}_{0.178}Cu^{+2}_{0.001})(Ca_{0.014}K_{0.024})O_{10}(OH)_2$, and hisingerite: $(Si_{3.634}Al_{0.351}Fe^{+3}_{0.015})(Al_{0.290}Fe^{+3}_{1.015}Mg_{0.242}Ti^{+4}_{0.007}Ni^{+2}_{0.737}Cr^{+3}_{0.117}Cu^{+2}_{0.002})(Ca_{0.027}K_{0.056})O_{10}(OH)_2$.

Weathering evolution from the coherent layer to the saprolitic layer at Angiquinho

The strongly serpentinized part of the coherent layer at Angiquinho is crosscut by veins filled with dolomite and magnesite. The serpentine is unweathered. The pyroxenes that are partly replaced by bastites contain an average of 0.3 percent Ni. In the saprolitic layer, the bastites are Ni rich (Ni occupies 1.5% of the octahedral sites). In the intermineral cracks, this bastite is replaced by a more aluminous and nickeliferous serpentine in which Ni occupies 8 percent of the octahedral sites. The average mineral formulas are: bastite: $(Si_{1.869}Al_{0.131})(Al_{0.050}Fe^{+2}_{0.327}Fe^{+3}_{0.074}Mg_{2.467}Cr^{+3}_{0.027}Ni^{+2}_{0.045})O_5(OH)_4$, and serpentine: $(Si_{1.987}Al_{0.013})(Al_{0.284}Fe^{+2}_{0.401}Fe^{+3}_{0.043}Mg_{1.839}Cr^{+3}_{0.028}Ni^{+2}_{0.234})O_5(OH)_4$.

At the top of the saprolitic layer, primary rock textures are still preserved (Fig. 8E). Recognizable relict pyroxenes are replaced by bastites and occur in a serpentine-rich gray-green matrix that contains 2 percent Ni. The rims of these altered pyroxenes, however, consist of a more aluminous and nickeliferous serpentine in which Ni occupies 10 percent of the octahedral sites. This phase has the average formula of: $(Si_{1.777}Al_{0.223})(Al_{0.267}Fe^{+3}_{0.430}Mg_{1.730}Cr^{+3}_{0.025}Ni^{+2}_{0.298})O_5(OH)_4$. The carbonate that was present in the coherent layer is replaced by garnierite which, in turn, may be replaced higher in this layer by asbolane having an average of 19 percent Ni.

The weakly serpentinized part of the coherent layer contains veins filled with garnierite. This garnierite is similar to the deweylite studied by Bish and Brindley (1978), but it has a higher Ni content (Ni occupies 15% of the octahedral sites in the serpentine and 32% in the kerolite). Along cracks, the hydrothermal alteration of pyroxene produced a mixture of bastite and chlorite-vermiculite that is similar to the mixed layer clays studied by Ostrowicki (1965) and Noack and Colin (1986). These hydrothermal phases are Ni enriched, with Ni respectively occupying 4.5 and 5 percent of the octahedral sites. At the base of the overlying saprolitic layer, saponite pseudomorphously replaces pyroxene along cracks. Its average formula is: $(Si_{3.411}Al_{0.578}Fe^{+3}_{0.011})(Al_{0.078}Fe^{+3}_{0.728}Mg_{1.181}Cr^{+3}_{0.116}Mn^{+2}_{0.009}Ti^{+4}_{0.006}Ni^{+2}_{0.631})(Ca_{0.069}K_{0.018})O_{10}(OH)_2$. This Fe saponite has 20 percent of its octahedral sites occupied by Ni and may be bordered by ferruginous oxyhydroxides that average 5 percent Ni (Fig. 8D).

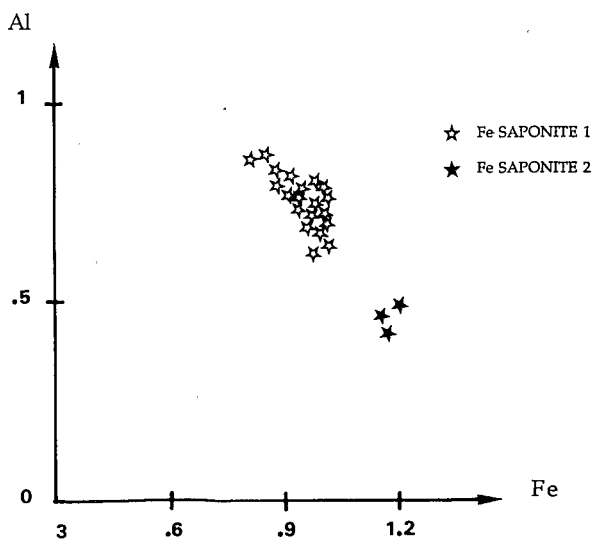

FIG. 7. Al and Fe variations in Fe saponite from the coherent layer at Jacuba.

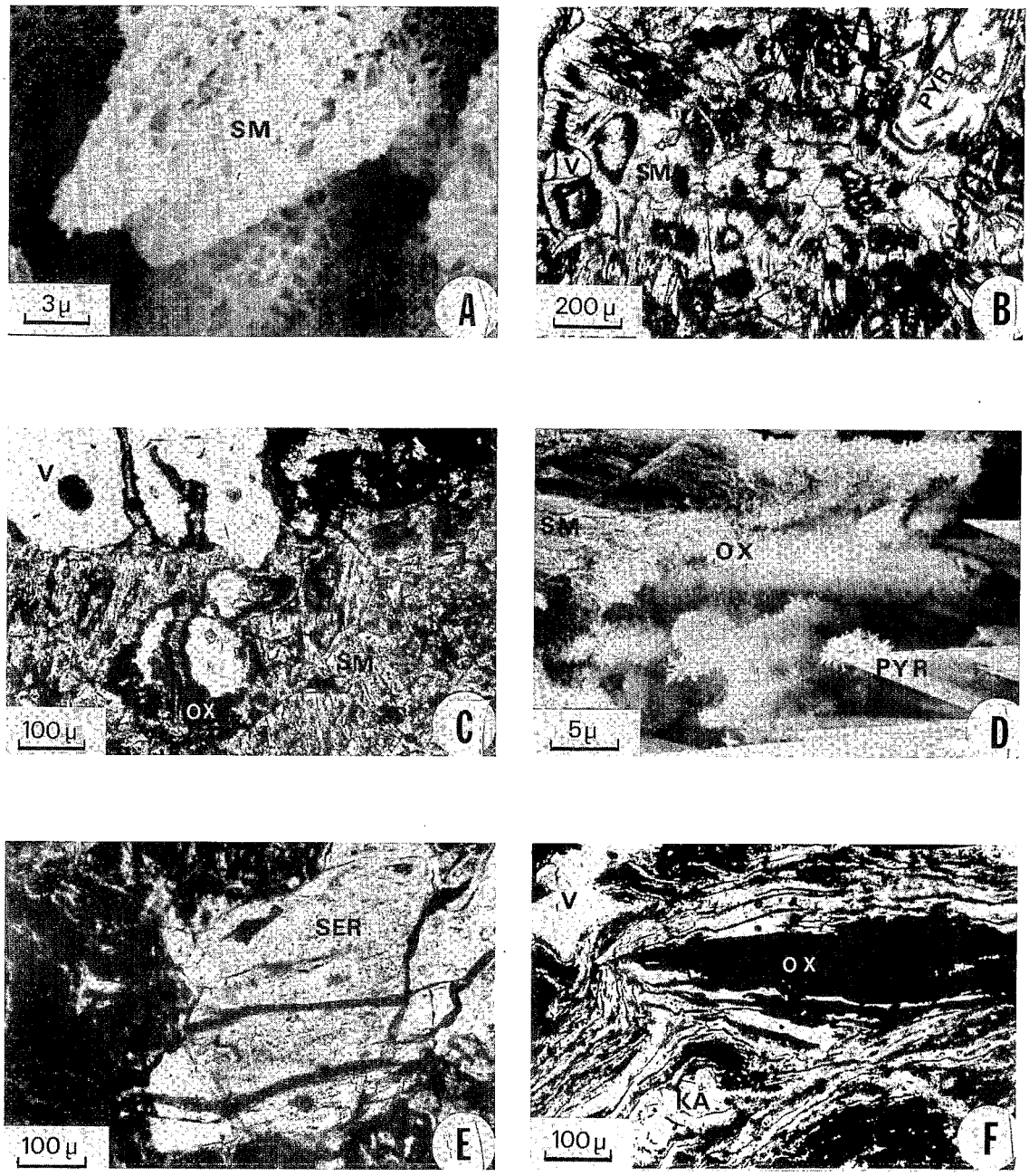

FIG. 8. A. Pyroxene replaced by smectite (SM) with preservation of tooth-shaped parent minerals. Scanning electron photomicrograph. B. Smectite (SM) formed at the expense of pyroxene (PYR) by centripetal alteration. V = void, OX = Fe oxyhydroxide. Thin section under crossed polars. C. The relicts of pyroxene are obliterated (V = void) and reveal aureoles of ferruginous oxyhydroxide (OX). SM = smectite. Thin section under crossed polars. D. Smectite (SM) bordered by ferruginous oxyhydroxide (OX). PYR = pyroxene. Scanning electron photomicrograph. E. Weathered serpentine (SER) with preservation of the parental texture. Thin section under crossed polars. F. Weathering of smectite and serpentine into kaolinite (KA) and ferruginous oxyhydroxide (OX). Thin section under crossed polars.

Although the original shapes of pyroxenes are still preserved, the more extensively weathered upper parts of the saprolitic layer contain relict pyroxenes that are extensively replaced by a greenish phyllosilicate. This is an Fe montmorillonite in which Ni occupies 9.3 percent of the octahedral sites. Its aver-

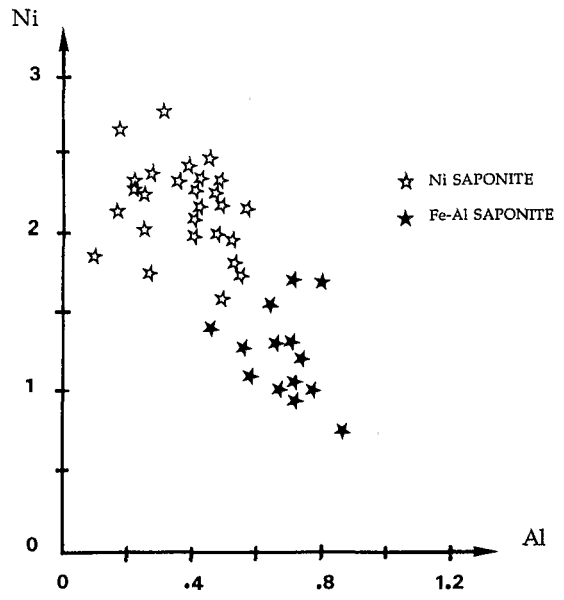

FIG. 9. Ni and Al variations in Ni saponite and Fe-Al saponite from the saprolitic layer at Jacuba.

age formula is: $(Si_{3.842}Al_{0.158})(Al_{0.349}Fe^{+3}_{1.147}Mg_{0.399}Cr^{+3}_{0.087}Ti^{+4}_{0.008}Ni^{+2}_{0.286})(Ca_{0.003}K_{0.001})O_{10}(OH)_2$.

At the top of the saprolitic layer, the original rock texture is destroyed. The smectite matrix is cut by asbolane-filled veins and consists of Fe montmorillonite and Al montmorillonite. The Fe-rich smectite is similar to that which occurs lower in the profile, but it has less nickel (Ni occupies 8% of the octahedral sites). The Al-rich montmorillonite has 9.3 percent of its octahedral sites occupied by Ni and has a average formula of: $(Si_{3.844}Al_{0.156})(Al_{0.838}Fe^{+3}_{0.535}Mg_{0.348}Cr^{+3}_{0.217}Ti^{+4}_{0.031}Ni^{+2}_{0.279})(Ca_{0.002}K_{0.004})O_{10}(OH)_2$.

Formation of the clayey ferruginous layers

At both Jacuba and Angiquinho, the clayey ferruginous layer is red-purple in color and is composed of a matrix of clayey and ferruginous material that is cut by veins filled with asbolane. The clayey matrix consists of small crystals of kaolinite (Fig. 8F), while the reddish ferruginous matrix consists essentially of goethite and kaolinite. The Ni content of the matrix is 0.2 to 0.3 percent.

Nickel Cycle in the Weathering Process

The two different weathering sequences and the manner in which nickel is transferred among minerals is summarized in Figures 10 and 11.

Jacuba

At Jacuba the parent pyroxenite contains about 0.1 percent nickel. In the coherent zone, during the first stages of weathering, the bulk volumes remain unchanged, but the Ni content, and therefore the absolute abundance of Ni, increases. In this zone, the abundance of Ni and the density of fractures are important in controlling the formation of secondary phyllosilicates from pyroxene. Where there are few fractures, the secondary phyllosilicate is an Fe saponite with Ni occupying 46 percent of the octahedral sites. Where fractures are abundant, the secondary phyllosilicates are a mixture of Fe saponite and a pimelite in which Ni respectively occupies 32.5 and 84 percent of the octahedral sites.

In the overlying saprolitic layer, the Fe saponites that formed during the first stages of weathering lose nickel (Ni occupies 41% of the octahedral sites) and change progressively to Fe-Al saponites. In contrast, weathering of pyroxenes in this zone results in the formation of very Ni-rich saponites in which Ni occupies 68 percent of the octahedral sites. Compared to the weakly fractured areas of the underlying coherent layer, there is a greater absolute increase of Ni in the saprolitic zone. Some of the nickel comes from the overlying clayey layer.

In the overlying clayey layer, the absolute abundance of nickel decreases. The nature of this decrease depends on the different supergene phyllosilicates

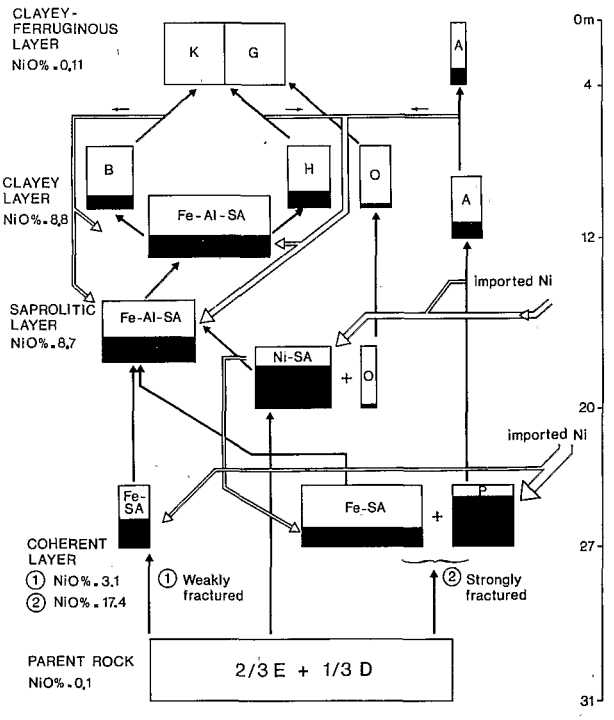

FIG. 10. Nickel cycle in the Jacuba weathering profile. A = asbolane, B = beibellite, D = diopside, E = enstatite, Fe-SA = Fe saponite, Fe-Al-SA = Fe-Al saponite, G = goethite, H = hisingerite, K = kaolinite, Ni-SA = Ni saponite, O = Fe-oxyhydroxyde, P = pimelite, ■ = approximate proportion of Ni in octahedron coordination, ⇒ = Ni transfer (the width of arrows is approximately proportional to the amount of Ni moved).

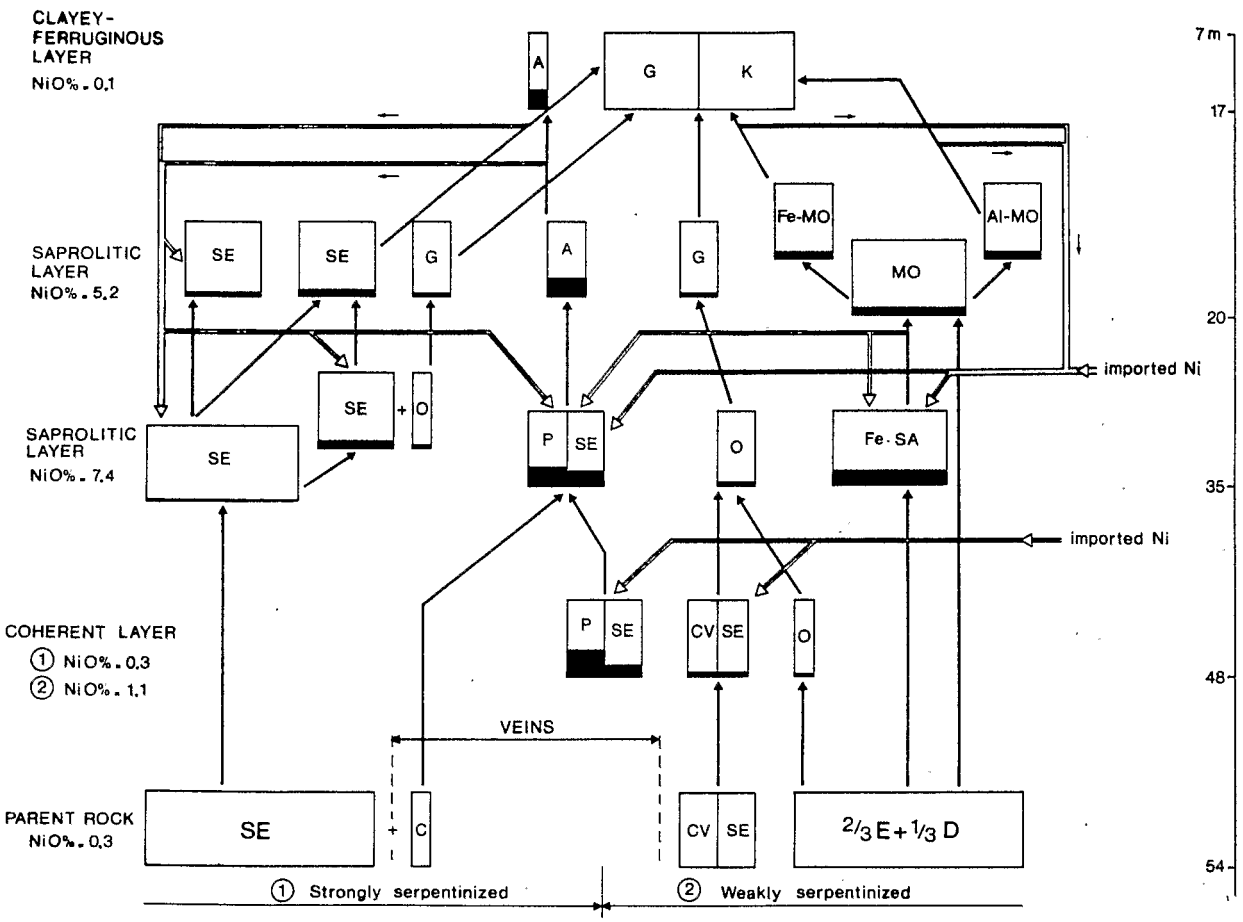

FIG. 11. Nickel cycle in the Angiquinho weathering profile. A = asbolane, Al-MO = Al montmorillonite, CA = carbonate, CV = chlorite-vermiculite, D = diopside, E = enstatite, Fe-MO = Fe montmorillonite, Fe-SA = Fe saponite, G = goethite, K = kaolinite, MO = montmorillonite, O = Fe oxyhydroxyde, P = pimelite. ■ = approximate proportion of Ni in octahedron coordination, A → B = replacement of A by B, ⇒ = Ni transfer (the width of arrows is approximately proportional to the amount of Ni moved).

which formed and on where alteration occurs. At the rims of pyroxene grains, Fe-Al saponite (having 41% Ni in its octahedral sites) progressively loses nickel until its Ni content is about 29 percent of the octaedral sites. At that point, it is replaced by hisingerite in which Ni occupies 24 percent of the octahedral sites. In the core of the pyroxene grains, the Ni saponite containing 68 percent Ni in its octahedral sites is first altered to an Fe-Al saponite having 29 percent Ni and then to a mixture of beidellite having 20 percent Ni in octahedral sites and kaolinite. As a result, weathering produces ferruginous-rich zones along cracks and grain boundaries, and concentrations of aluminous alteration at the cores of the pyroxenes.

Intense leaching of Ni occurs in the overlying clayey ferruginous layer. This is accompanied by an increase in the segregation of aluminous and ferruginous weathering products which occurs along with the transformation of beidellite to kaolinite, and of hisingerite to kaolinite plus goethite. Many of the veins crosscutting the layer are filled with asbolane and have an average of 26 percent Ni.

Angiquinho

As at Jacuba, the nickel content of unweathered pyroxenite at Angiquinho is almost zero. Unlike Jacuba, the parent pyroxene is partly serpentinized and the nickel content of the serpentine is about 0.1 percent.

In strongly serpentinized areas, the mesh serpentine and bastite are scarcely altered during the first weathering stage. However, in weakly serpentinized zones three changes occur during the formation of the coherent layer. The first is the filling of voids with garnierite (pimelite with 32% Ni and serpentine with 15% Ni in octahedral sites). The second is the pre-

cipitation in cleavages and cracks of pyroxene of poorly crystallized iron oxyhydroxides having 1.3 percent nickel. The third is the increase in nickel content of hydrothermal bastites and chlorite-vermiculite, respectively, to 4.6 percent and 5 percent of their octahedral sites. The result is an absolute increase of nickel in the coherent layer of about 190 percent.

At the base of the saprolitic layer, the weathering of weakly serpentinized pyroxene increases. The main mechanisms are (1) filling voids with garnierite (kerolite and serpentine) which is less nickeliferous than that formed in the underlying layer; (2) pseudomorphic replacement of pyroxene by Fe saponite which contains 20 percent Ni in its octahedral sites and which is surrounded by poorly crystallized iron oxyhydroxides that have 5 percent Ni; and (3) increasing Ni enrichment of serpentine to an Ni content of 8 percent in octahedral sites. The base of the saprolitic layer shows an absolute increase in nickel of 1,100 percent compared to the parent values.

At the top of the saprolitic layer, the iron oxyhydroxides alter to goethite that has 4 percent nickel. The pyroxene relicts and the Fe saponites are transformed into two types of smectite: an Fe smectite with 8 percent Ni in its octahedral sites and an Al smectite with 9.2 percent Ni. During this change, there is a loss of nickel to the underlying layers. The original mesh serpentine is altered to a serpentine matrix having 2 percent Ni. The original bastite remains largely unchanged but has nickel enrichment in its rims. The mean NiO content of the top of the saprolitic layer is near 5.2 percent, which reflects a loss of nickel that has moved downward into underlying parts of the profile.

As at Jacuba, the clayey ferruginous layer at the top of the weathering profile consists of kaolinite (Ni content of 0.3%) and goethite (Ni content of 0.2%) that is associated with asbolane (Ni content of 19%).

Discussion

Weathering of pyroxenes

During the first stage, the rates of weathering of clinopyroxene and orthopyroxene differ. Colin et al. (1985) showed that enstatite weathers twice as rapidly as diopside to form Fe saponite. Eggleton (1986) suggests that the slower weathering of clinopyroxene results from its better lattice fit with talclike layers. However, the phyllosilicate matrix produced from these two parent minerals has the same chemical composition. This indicates that short distance exchange of chemical components has occurred between parent minerals. Similar chemical exchange was noted by Golightly and Arancibia (1979), Nahon et al. (1982a and b), and Paquet et al. (1987).

The weathering product of the two pyroxenes is a smectite in which Ni occupies 10 to 84 percent of the octahedral sites. This occupancy is higher than that reported by Eggleton (1975), Pion (1979), Nakajima and Ribbe (1980), Eggleton and Boland (1982), and Nahon and Colin (1982). Ni-rich smectite can also form from weathering of olivines and serpentines (Trescases, 1975; Esson and Dos Santos, 1978; Golightly, 1981; Nahon et al., 1982b), but such occurrences are rare. It appears that in the lateritic weathering of ultrabasic rocks pyroxene is the main parent mineral leading to the formation of smectite.

Two hypotheses can be given to explain this fact. First, during the incongruent dissolution of pyroxene, the chains of tetrahedra and/or octahedra are probably not entirely disorganized; this promotes the nucleation of smectite which has a lattice fit with the pyroxene structure. In contrast, incongruent dissolution of olivine leads to the formation of amorphous silica and poorly crystallized ferric oxyhydroxides. Because of the dimensional misfit between clay minerals and olivine, little clay develops on the olivine (Eggleton, 1986).

Second, in the case of the congruent dissolution of parent minerals, smectite precipitates directly from the weathering aqueous solution (Berner et al., 1980; Berner and Schott, 1982). Rates of chemical weathering of parent minerals are different for olivine, pyroxene, and serpentine. Olivine weathers first, and since they are Mg rich, their weathering products are Mg-bearing smectites. These smectites rapidly dissolved with increasing weathering. In contrast, Al-bearing pyroxene weathers more slowly and produces an Al-bearing smectite which is more stable under lateritic conditions than Mg-bearing smectite. Serpentine weathers even more slowly than olivine and pyroxene. Where the porosity is high and the waters are diluted, both Al- and Mg-bearing smectite are unstable. In this case, serpentine weathers directly to kaolinite and goethite. However, in some climates, this is not the case. Serpentine weathers to smectite in arid climates (e.g., Senegal: Blot et al., 1976; northeast Brazil: Melfi et al., 1980; Trescases et al., 1987; and Australia: Golightly, 1981) and in some temperate climates (Fontanaud, 1982).

In the Niquelandia area, the smectite formed from pyroxenes is Mg-Ni bearing (trioctahedral) in the early stage of weathering and Fe-Al bearing (dioctahedral) in later stages. This succession was predicted by Paquet et al. (1983) in West African examples. In Niquelandia, the size and abundance of voids and fractures in the parent rock control the rate of water movement and partly control the composition of the smectites; however, the composition of smectite is predominantly controlled by the chemical composition of the ground water. As long as primary pyroxenes are present, the solution will be saturated in Mg and the formation of trioctahedral smectite is favored. When all the pyroxenes have been weathered, the

amount of dissolved Mg decreases and the Mg content of the ground water is lowered. At this time trioctahedral smectite begins to change to dioctahedral smectite.

Toward the top of the lateritic profile, dioctahedral smectite, in turn, breaks down to kaolinite plus goethite. This breakdown is accompanied by a loss of parent-rock textures. Kaolinite is abundant in the upper part of the Niquelandia profiles, and because the structure of kaolinite does not permit Ni substitution, nickel is removed from this zone. This precludes the formation of Ni oxide ores at the top of lateritic profiles. The absence of an Ni oxide-rich top differs from the weathering profiles commonly developed on dunitic rock. The lack of aluminum in dunites does not enable kaolinite to form and therefore makes it possible for nickel-rich iron hydroxide accumulations to form at the profile top. These accumulations make up the ore in many of the better known deposits (Golightly, 1981).

Behavior of nickel in the Niquelandia weathering profiles

At Niquelandia, the nickel is released by weathering of olivine, pyroxene, and serpentine minerals. It accumulates at the base of profiles in authigenic weathering products (smectite originating from pyroxenes, garnierite filling cracks) and in still-unweathered serpentine grains. With increasing weathering, smectite, garnierite, and serpentine crystals are destabilized. The nickel is then released once again and is redistributed in newly formed phyllosilicates at the base of the profiles. This accumulation is more intense where the rock is highly fractured, as at Jacuba. As a result, the main Ni-bearing minerals are trioctahedral smectites. This contrasts with occurrences in New Caledonia (Trescases, 1975) where weathering did not produce smectite and the Ni was trapped in serpentine.

The smectites at Jacuba are richer in nickel than those of Angiquinho. This is due to the geomorphologic setting of pyroxenite at Jacuba which is a suspended valley between hills of dunite. In this topographically low position, ground waters are enriched in nickel that has been released from the nearby dunite. At Angiquinho, pyroxenite is much less abundant than at Jacuba, and it occurs as veins in dunite and peridotite. The pyroxenite in the veins weathers into smectite, and percolating solutions laterally bring in Ni from the adjacent dunite.

Comparisons with known lateritic nickel occurrences

The nickeliferous lateritic deposits of the Niquelandia area are essentially Ni silicate deposits and are very different from other dunite-derived Ni-bearing deposits in the Philippines (Frasché, 1941; Santos-Ynigo, 1964), Venezuela (Jurkovic, 1953), Guinea (Millot and Bonifas, 1955), Australia (Turner, 1968), and South Africa (de Waal, 1971), where most Ni occurs in goethite. On the other hand, silicate and oxide Ni deposits are well known in Senegal (Blot et al., 1976), New Caledonia (Trescases, 1975, 1979), Brazil (Esson and Dos Santos, 1978), Indonesia (Kuhnel et al., 1978), and Australia (Golightly, 1981). However, the secondary nickel silicates (garnierite and smectite) in those deposits result from the weathering of olivine and serpentine, not from pyroxene as at Jacuba and Angiquinho. Moreover, the Ni content of such olivine- and serpentine-derived smectites is less than 5 percent. Ni-bearing smectites have also been described from Brazil and the Ivory Coast (Colin et al., 1980; Melfi et al., 1980; Nahon and Colin, 1982; Nahon et al., 1982b) as pseudomorphs after pyroxenes. However, these phyllosilicates have an octahedral Ni content that is less than 7 percent. Thus, the weathering of ultramafic rocks of Niquelandia constitutes an exceptional occurrence of high Ni concentration in secondary phyllosilicates. This is especially the case at Jacuba, where lateritic weathering, geologic setting (interlayered dunite and pyroxenite), and geomorphology (a suspended valley in pyroxenite surrounded by dunite hills) combine to yield extremely high Ni contents.

Acknowledgments

The authors are particularly indebted to E. Merino (University of Bloomington, Indiana) for the critical review of the text and for improving the English. Their thanks are also due to the Niquel Tocantins Cie for its interest and its contribution to this study. The manuscript was greatly improved by comments from *Economic Geology* reviewers.

REFERENCES

Araujo, V. A., de Mello, J. C. R., and Oguino, K., 1972, Projeto Niquelandia. Relatorio final. Convenio Departemento National de Producao Mineral-Compania de Pesquisa de Recurso Minerais Goiana, 224 p.

Berner, R. A., and Schott, J., 1982, Mechanism of pyroxene and amphibole weathering. II. Observation of soil grains: Am. Jour. Sci., v. 282, p. 1214–1231.

Berner, R. A., Sjoberg, E. L., Velbel, M. A., and Krom, M. D., 1980, Dissolution of pyroxenes and amphiboles during weathering: Science, v. 207, p. 1205–1206.

Bish, D. L., and Brindley, G., 1978, Deweylites, mixtures of poorly crystaline serpentine and talc like minerals: Mineralog. Mag., v. 42, p. 75–79.

Blot, A., Leprun, J. C., and Pion, J. C., 1976, Originalite de l'altération et du cuirassement des dykes basiques dans le massif de granite de Sanaga (Senégal Oriental): Soc. Geol. France Bull., Ser. 7, v. 18, no. 1, p. 45–49.

Brigatti, M. F., 1981, Hisingerite: a review of its crystal chemistry: Internat. Clay Conf., 7th, Bologna and Pavia, Italy, 6–12 September, 1981, Proc., p. 97–110.

Colin, F., 1985, Etude petrologique des altérations de pyroxenite du gisement nickélifère de Niquélandia (Brésil): Travaux et documents Microédités ORSTOM. F17, 137 p.

Colin, F., Parron, C., Bocquier, G., and Nahon, D., 1980, Nickel and chromium concentrations by chemical weathering of pyroxenes and olivines, *in* Metallogeny of mafic and ultramafic complexes: UNESCO, Internat. Symposium, Athens, 1980, Proc., v. 2, p. 56–66.

Colin, F., Noack, Y., Trescases, J. J., and Nahon, D., 1985, L'altération latéritique débutante des pyroxénites de Jacuba, Niquélandia, Brésil: Clay Minerals, v. 20, p. 93–113.

Danni, J. C. M., Fuck, R. A., and Leonardos, O. H., 1982, Archaean and lower Proterozoic units in central Brazil: Geol. Rundschau, v. 71, p. 291–317.

Decarreau, A., Colin, F., Herbillon, A., Manceau, A., Nahon, D., Paquet, H., Trauth-Badaud, D., and Trescases, J. J., 1987, Domain segregation in Ni-Fe-Mg-smectites: Clays and Clay Minerals, v. 35, p. 1–10.

Dungan, M. A., 1979a, A microprobe study of antigorite and some serpentine pseudomorphs: Canadian Mineralogist, v. 17, p. 771–784.

—— 1979b, Bastite pseudomorphs after orthopyroxene, clinopyroxene and tremolite: Canadian Mineralogist, v. 17, p. 729–740.

Eggleton, R. A., 1975, Nontronite topotaxial after hedenbergite: Am. Mineralogist, v. 60, p. 1063–1068.

—— 1986, The relations between crystal structure and silicate weathering rates, *in* Colman, S. T., and Dethier, D. P., ed., Rates of chemical weathering of rocks and minerals: New York, Academic Press, p. 21–40.

Eggleton, R. A., and Boland, J. N., 1982, The weathering of enstatite to talc through a series of transitional phases: Clays and Clay Minerals, v. 30, p. 11–20.

Esson, J., and Dos Santos, L. W., 1978, The occurrence, mineralogy and chemistry of some garnierites of Brazil: Bur. Recherches Geol. Min. Bull. v. 3, p. 263–274.

Figueiredo, A. N. de, Motta, J., and Marques, V. J., 1975, Estudo comparativo entre os complexos de Barro Alto e do Tocantins, Goias: Revista Brasileira Geociencias, v. 5, p. 15–29.

Fontanaud, A., 1982, Les faciès d'altération supergène des roches ultrabasiques: Unpub. thèse, 3rd cycle, Univ. Poitiers, 103 p.

Frasché, D. F., 1941, Origin of the Surigao iron ores: ECON. GEOL., v. 46, p. 280–305.

Girardi, V. A. V., Kawashita, R., and Cordani, 1978, Algumas consideraçoes sobre a evolucao geologica da regiao de Cana Brava a partir de dados géocronologicos: Cong. Brasileiro Geologia, 30th, Recife, Anais, v. 1, p. 337–348.

Girardi, V. A. V., Rivalenti, G., and Sinigoi, S., 1986, The petrogenesis of the Niquelandia layered basic-ultrabasic complex, central Goias, Brazil: Jour. Petrology, v. 27, p. 715–744.

Golightly, J. P., 1981, Nickeliferous laterite deposits: ECON. GEOL. 75TH ANNIV. VOL., p. 710–735.

Golightly, J. P., and Arancibia, O. N., 1979, The chemical composition and infrared spectrum of nickel- and iron-substituted serpentine from a nickeliferous laterite profile, Soroako, Indonesia: Canadian Mineralogist, v. 17, p. 719–728.

Jurkovic, I., 1953, Some geochemical aspects about the genesis of the nickel deposits Loma de Hierro (Venezuela): Geol. Vjesnik., v. 17, p. 103–112.

Kûhnel, R. A., Roorda, H. J., and Steesma, J. J. S., 1978, Distribution and partitioning of elements in nickeliferous laterites: Bur. Recherches Geol. Min. Bull., v. 3, p. 191–206.

Leonardos, J. R., Danni, J. C. M., Pedroso, A. C., and Schmaltz, W. H., 1982, Lateritic nickel deposit of Niquelandia, GO: II Internat. seminar on Laterisation Processes, 2nd, Saõ-Paulo, Brazil, July 4–12, 1982, Proc., p. 91–107.

Melfi, A. J., Trescases, J. J., and Barros de Oliviera, S. M., 1980, Les latérites nickélifères du Brésil: ORSTOM, Cahiers Ser. Géol., v. 11, p. 1232–1243.

Millot, G., and Bonifas, M., 1955, Transformations isovolumétriques dans les phénomènes de latéritisation et de bauxitisation: Alsace Lorraine Service Carte Géol. Bull., v. 8, p. 3–20.

Nahon, D., and Colin, F., 1982, Chemical weathering of orthopyroxenes under lateritic conditions: Am. Jour. Sci., v. 282, p. 1232–1243.

Nahon, D., Colin, F., and Tardy, Y., 1982a, Formation and distribution of Mg, Fe, Mn-smectites in the first stages of the lateritic weathering of forsterite and tephroite: Clay Minerals, v. 17, p. 339–348.

Nahon, D. B., Paquet, H., and Delvigne, J., 1982b, Lateritic weathering of ultramafic rocks and the concentration of nickel in the western Ivory Coast: ECON. GEOL., v. 77, p. 1159–1175.

Nakajima, Y., and Ribbe, P. H., 1980, Alteration of pyroxenes from Hokkaido, Japan, to amphibole, clays and other biopyriboles: Neues Jahrb. Mineralogie, v. 6, p. 258–268.

Noack, Y., and Colin, F., 1986, Chlorites and chloritic mixed layer minerals in profiles on ultrabasic rocks from Moyango (Ivory Coast) and Angiquinho (Brazil): Clay Minerals, v. 21, p. 171–182.

Ostrowicki, B., 1965, Mineraly niklu strefy wie trzenia serpentyritow w Szklarach [Nickel minerals in the weathering zone of serpentines at Szklary, lower Silesia]: Polska Acad. Nauk., Oddz., Krakow., Prace Min., v. 1, p. 7–92.

Paquet, H., Duplay, J., Nahon, D., Tardy, Y., and Millot, G., 1983, Analyses chimiques de particules isolées dans les populations de minéraux argileux: Acad. Sci. [Paris], Comptes Rendus, v. 296, sér. II, p. 699–704.

Paquet, H., Colin, F., Duplay, J., Nahon, D., and Millot, G., 1987, Ni, Mn, Zn, Cr-smectites, early and effective traps for transition elements in supergene ore deposits, *in* Rodriguez, C., and Tardy, Y., eds., Geochemistry and minerals formation in the earth surface: Madrid, Consejo Superior Inv. Cient., p. 188–201.

Pecora, W. T., 1944, Nickel silicate associated nickel-cobalt-manganese oxide deposits near Sao José dos Tocantins, Goias, Brazil: U. S. Geol. Survey Bull. 935 E, p. 247–305.

Pedroso, A. C., and Schmaltz, W. H., 1981, Jazimentos de niquel lateritico de Niquelandia, Goias: Simposio Geologie Centro Oeste Brasileiro, v. 1, p. 185–207.

Pion, J. C., 1979, Altération des massifs cristallins basiques en zone tropicale sèche; Étude de quelques toposéquence en Haute Volta: Univ. Louis Pasteur Strasbourg, Inst. Géologie, Mem. 57, 220 p.

Rivalenti, G., Girardi, V. A. V., Sinigoi, S., Rossi, A., and Siena, F., 1982, The Niquelandia mafic-ultramafic complex of central Goias, Brazil: Petrological considerations: Rev. Brasileira Geocienc., v. 12, p. 380–391.

Santos-Ynigo, L., 1964, Distribution of iron, alumina and silica in the Pujada Laterite of Mati, Davao Province, Mindanao Island (Philippines): Internat. Geol. Cong., 22nd, New Dehli, 1964, Proc., v. 14, p. 126–141.

Trescases, J. J., 1975, L'évolution géologique supergéne des roches ultrabasiques en zones tropicale. Formation des gisements nickélifères de Nouvelle Calédonie: ORSTOM Mem., 259 p.

—— 1979, Remplacement progressif des silicates par les hydoxydes de fer et de nickel dans les profils d'altération tropicale des roches ultrabasiques. Accumulation résiduelle et épigénie: Strasbourg and Sci. Géol. Bull., v. 32, p. 181–188.

Trescases, J. J., Dino, R., and Oliveira, S. M. B., 1987, Un gisement de nickel en zone semi-aride: Sao Jao do Piaui (Brésil) *in* Rodriguez, C., and Tardy, Y., eds., Geochemistry and mineral formation in the earth surface: Madrid, Consejo Superior Inv. Cient., p. 273–288.

Turner, R. A., 1968, The distribution and association of nickel in the ferruginous zones of laterites of the Giles Complex, Australia: Australian Mineral Devel. Lab. Bull., v. 5, p. 76–93.

Waal, S. A. de, 1971, South African nickeliferous serpentinites: Minerals Sci. Eng., v. 3, p. 32–45.

Wicks, F. J., and Wittaker, E. J. W., 1977, Serpentine texture and serpentinization: Canadian Mineralogist, v. 15, p. 459–488.